Computers, Materials & Continua

Tech Science Press

Doi:10.32604/cmc.2026.076690

ARTICLE

Optimizing Routing Algorithms for Next-Generation Networks: A Resilience-Driven Framework for Space-Air-Ground Integrated Networks

Peiying Zhang[1,2], Yihong Yu[1,2], Jia Luo[3,4,*], Nguyen Gia Ba[5], Lizhuang Tan[6,7] and Lei Shi[8]

[1]Qingdao Institute of Software, College of Computer Science and Technology, China University of Petroleum (East China), Qingdao, 266580, China
[2]Shandong Key Laboratory of Intelligent Oil & Gas Industrial Software, Qingdao, 266580, China
[3]College of Economics and Management, Beijing University of Technology, Beijing, 100124, China
[4]Chongqing Research Institute, Beijing University of Technology, Chongqing, 401121, China
[5]Faculty of Information Technology, Hung Yen University of Technology and Education, Hung Yen, 17000, Vietnam
[6]Key Laboratory of Computing Power Network and Information Security, Ministry of Education, Shandong Computer Science Center (National Supercomputer Center in Jinan), Qilu University of Technology (Shandong Academy of Sciences), Jinan, 250014, China
[7]Shandong Provincial Key Laboratory of Computing Power Internet and Service Computing, Shandong Fundamental Research Center for Computer Science, Jinan, 250014, China
[8]State Key Laboratory of Media Convergence and Communication, Communication University of China, Beijing, 100024, China

*Corresponding Author: Jia Luo. Email: jialuo@bjut.edu.cn

Received: 25 November 2025; Accepted: 04 January 2026; Published: 12 March 2026

ABSTRACT: Next-Generation Networks (NGNs) demand high resilience, dynamic adaptability, and efficient resource utilization to enable ubiquitous connectivity. In this context, the Space-Air-Ground Integrated Network (SAGIN) architecture is uniquely positioned to meet these requirements. However, conventional NGN routing algorithms often fail to account for SAGIN's intrinsic characteristics, such as its heterogeneous structure, dynamic topology, and constrained resources, leading to suboptimal performance under disruptions such as node failures or cyberattacks. To meet these demands for SAGIN, this study proposes a resilience-oriented routing optimization framework featuring dynamic weighting and multi-objective evaluation. Methodologically, we define three core routing performance metrics, quantified through a four-dimensional model, encompassing robustness R_d, resilience R_r, adaptability R_a, and resource utilization efficiency R_u, and integrate them into a comprehensive evaluation metric. In simulated SAGIN environments, the proposed Multi-Indicator Weighted Resilience Evaluation Algorithm (MIW-REA) demonstrates significant improvements in resilience enhancement, recovery acceleration, and resource optimization. It maintains 82.3% service availability even with a 30% node failure rate, reduces Distributed Denial of Service (DDoS) attack recovery time by 43%, decreases bandwidth waste by 23.4%, and lowers energy consumption by 18.9%. By addressing challenges unique to the SAGIN network, this research provides a flexible real-time solution for NGN routing optimization that balances resilience, efficiency, and adaptability, advancing the field.

KEYWORDS: Space-air-ground integrated network; next-generation networks; routing optimization; resilience-driven routing; dynamic weighting; multi-metric assessment

1 Introduction

With the acceleration of global digitalization, the Space-Air-Ground Integrated Network (SAGIN) has emerged as a core innovation paradigm for Next-Generation Networks (NGNs) [1–3].

However, SAGIN's multi-domain integration introduces substantial network resilience (NR) challenges [4]. NR refers to a system's ability to maintain or rapidly restore critical functions when subjected to disruptions such as cyberattacks, hardware failures, or natural disasters—a capability vital for mission-critical scenarios [5–8]. The traditional isolated operation of terrestrial and satellite networks exposes clear weaknesses during large-scale disruptions, terrestrial networks are vulnerable to physical damage, while satellite networks face signal attenuation and orbital congestion issues [9]. Although SAGIN enhances fault tolerance and redundancy through cross-domain collaboration, its heterogeneous dynamic characteristics, including variable topology, fluctuating link quality, and multidimensional threats impose higher demands on resilience assurance [10,11].

NR as a key performance indicator, encompasses three core dimensions: survivability, self-healing capability, and resource utilization efficiency. Balancing these three is essential for the stable and efficient operation of SAGIN [12–14]. The urgent need for resilience in SAGIN stems from three aspects: node mobility and spatial distribution render centralized control impractical, necessitating reliance on autonomous distributed mechanisms; differences in multi-domain protocols, latency constraints, and failure modes demand a unified resilience assessment framework; and stringent requirements for communication reliability and low latency in applications like national defense and public safety, making resilience a strategic imperative [15,16]. Most resilience characterization methods fail to account for SAGIN's cross-domain interactions and dependencies, static models struggle to adapt to its dynamic characteristics, and some studies overlook the impact of resource utilization efficiency on long-term stability [17–19].

To address these gaps, this paper proposes a novel network resilience characterization theory tailored for SAGIN, constructing a quantitative model based on survivability, self-healing capability, and resource utilization efficiency, and designing a Multi-Indicator Weighted Resilience Evaluation Algorithm (MIWREA). By dynamically adjusting indicator weights in real-time based on network status and application demands, the algorithm enhances the flexibility and accuracy of resilience assessment, providing robust support for decision optimization.

2 SAGIN Resilience Modeling

2.1 Network Modeling

The topology of SAGIN can be modeled as a weighted directed graph $G = \{V, E, W\}$ [20], where V represents a node set comprising space-based nodes, air-based nodes, and ground-based nodes. The edge set E describes the connectivity relationships among interstellar links, air-ground links (GAL), and terrestrial links. The weight set W integrates three key parameters, link quality, transmission delay, and bandwidth capacity. As shown in Fig. 1, SAGIN's three-layer topology significantly enhances network connectivity [21–23]. Empirical data indicates that its connectivity rate improves from 82% to 98.7% ($p < 0.01$) compared to traditional architectures.

2.2 Resilience Modeling

NR is formally defined as the ability of a system to maintain an acceptable level of service performance $\Phi(t) \in [0,1]$ when subjected to a set of perturbing events $e \in E$, where E represents the space of all possible disruptive events, including cyber attacks, equipment failures, and environmental disturbances. We propose a four dimensional characterization model.

$$R = (R_d, R_r, R_a, R_u) \quad \forall t \in T \tag{1}$$

where T is the observation time window, R_d represents the robustness of the system, R_r denotes the recovery capability, R_a describes the adaptability and R_u measures the resource utilization efficiency.

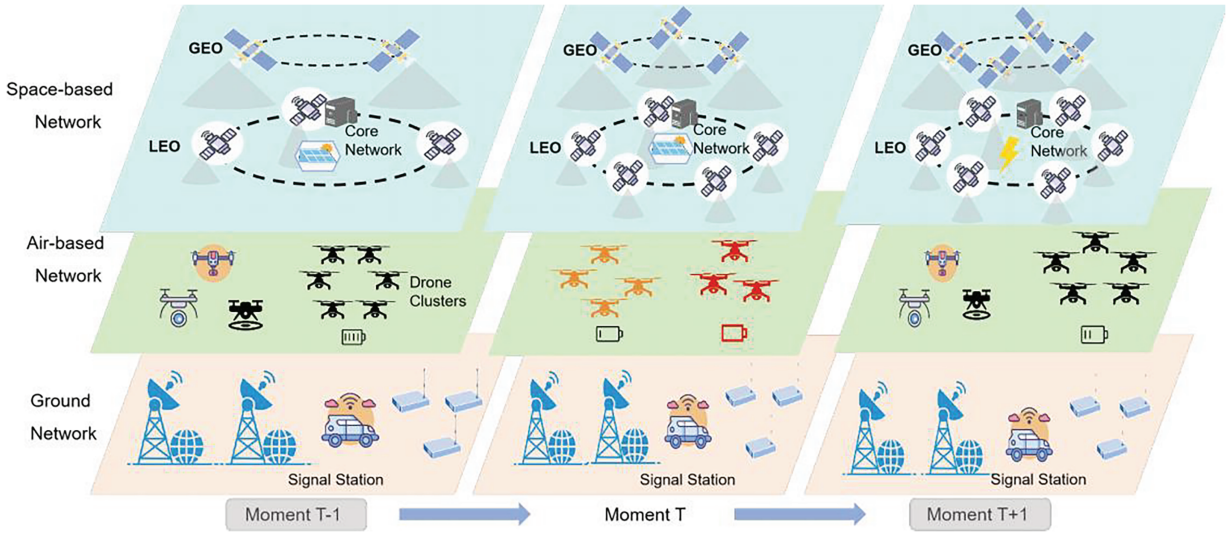

Figure 1: The topology of SAGIN

The four resilience dimensions dynamically influence routing through the following mechanisms: robustness-aware path selection, prioritizing high-redundancy paths when $R_d(t)$ falls below threshold θ_d, recovery-triggered rerouting, proactively switching to backup paths upon a sharp decline in $R_r(t)$, adaptability-driven topology adjustment, guiding topology reconfiguration and adjusting routing table update frequency based on $R_a(t)$ values, and resource-aware load distribution, controlling traffic allocation via $R_u(t)$ to avoid resource-saturated links.

2.2.1 Robustness Function

The robustness function $R_d(t)$ is defined as a piecewise function that characterizes the system's resistance capability.

$$R_d(t) = \begin{cases} 1 - \dfrac{\Phi_0 - \Phi(t)}{\Phi_0} & t < t_d \\ e^{-\lambda(t-t_d)} & t \geq t_d \end{cases} \tag{2}$$

where Φ_0 is the baseline performance level, t_d marks the onset time of disruption.

In SAGIN environments, the degradation rate parameter λ is dynamically adjusted based on cross-domain link availability:

$$\lambda(t) = \frac{1}{t_{1/2}} \ln 2 \cdot \left(1 + \alpha \cdot \frac{N_{\text{failed, cross-links}}(t)}{N_{\text{total, cross-links}}}\right) \tag{3}$$

where $\alpha = 0.3$ is an empirical coefficient, and $N_{\text{failed, cross-links}}(t)$ denotes the number of failed space-to-air or air-to-ground links at time t. This modification captures the cascading failure characteristic inherent to SAGIN.

2.2.2 Recovery Function

$R_r(t)$ represents the recovery function. The recovery function employs a sigmoidal model to characterize the rate and efficiency of network restoration following failures.

$$R_r(t) = \frac{1}{1 + e^{-k(t-t_{\text{rec}})}} \tag{4}$$

where k determines the steepness of recovery (higher values indicate faster restoration); t_{rec} represents the time required to achieve 50% functionality recovery.

$$\frac{dR_r(t)}{dt} = kR_r(t)\left(1 - R_r(t)\right) \tag{5}$$

This model captures the nonlinear recovery dynamics: initial slow response, accelerated mid-phase recovery, and eventual stabilization. Practical implementation requires parameter optimization based on availability of recovery resources, potential collision probability, e.g., satellite/Unmanned Aerial Vehicle (UAV) collision domain.

2.2.3 Adaptability Function

The adaptability function $R_a(t)$ quantifies the network's capability to dynamically reconfigure its topology and operational parameters.

$$R_a(t) = p_a(t) \cdot \left(1 - \frac{H(t)}{H_{\max}}\right) \tag{6}$$

where $p_a(t)$ is success probability of reconfiguration attempts, $H(t)$ is configuration entropy measuring system disorder.

$$H(t) = -\sum_{i=1}^{M} p_i(t) \log p_i(t) \tag{7}$$

$H_{\max} = \log M$ is maximum entropy for M available configuration states, entropy values indicate more ordered network states, corresponding to higher adaptability. For SAGIN, the concept of configuration entropy has been extended to encompass orbital periodicity and the dynamic characteristics of drone swarms:

$$H_{\text{SAGIN}}(t) = -\sum_{i=1}^{M} p_i(t) \log p_i(t) + \beta \cdot \sin\left(\frac{2\pi t}{T_{\text{orbit}}} + \phi\right) \tag{8}$$

where T_{orbit} is the orbital period of Low Earth Orbit (LEO) satellites, $\beta = 0.2$ adjusts the periodic influence, and ϕ is the phase offset. This formulation captures the predictable yet dynamic nature of SAGIN topology changes.

2.2.4 Resource Utilization Efficiency Function

The resource utilization efficiency function $R_u(t)$ quantifies the optimal allocation of network resources including bandwidth, CPU, and energy through a weighted geometric mean formulation.

$$R_u(t) = \prod_{j=1}^{n} \left(\frac{u_j(t)}{u_j^{\max}}\right)^{w_j} \tag{9}$$

where $u_j(t)$ represents the real-time utilization of resource j, $u_j^{\max}$ denotes its maximum capacity, and w_j are non-negatively weighted satisfying $\sum_{j=1}^{n} w_j = 1$.

The weighted geometric mean formulation is adopted for resource utilization efficiency assessment due to its inherent advantage in preventing single-resource bottlenecks. Unlike arithmetic mean approaches that allow high performance in one dimension to compensate for deficiencies in others, the geometric mean ensures balanced utilization across all resource types. This property is particularly crucial in SAGIN environments where heterogeneous resources (bandwidth, CPU, energy) must be coordinated efficiently. Additionally, the geometric mean's multiplicative nature naturally penalizes extreme underutilization of any single resource, thus promoting more sustainable resource allocation patterns in resource-constrained SAGIN operations.

2.2.5 Integrated Resilience Model

The Integrated Resilience Model $R_{\text{total}}(T)$ provides a comprehensive assessment by combining four key metrics-robustness, recovery capability, adaptability, and resource efficiency-through the integration formula.

$$R_{\text{total}}(T) = \frac{1}{T}\int_0^T \sum_{i=1}^{4} \omega_i(t) R_i(t) dt \tag{10}$$

the adaptive weighting mechanism $\omega_i(t)$ enables dynamic resource allocation and system optimization in line with journal focus areas.

$$\omega_i(t) = \frac{\sigma_i^{-2}(t)}{\sum_{i=1}^{4} \sigma_i^{-2}(t)} \tag{11}$$

where $\sigma_i^{-2}(t)$ represents the variance of metric i in a sliding time window. This weighting scheme automatically assigns greater importance to more stable metrics with lower variance, ensuring that the model prioritizes consistent optimization.

The interdependence between space, air, and ground domains creates unique resilience characteristics not found in single-domain networks. We model this coupling through a cross-domain influence matrix.

$$C(t) = \begin{bmatrix} c_{ss} & c_{sa} & c_{sg} \\ c_{as} & c_{aa} & c_{ag} \\ c_{gs} & c_{ga} & c_{gg} \end{bmatrix}, \quad \text{where } c_{xy}(t) = \frac{\text{Active links between domains } x \text{ and } y}{\text{Total possible links}} \tag{12}$$

The integrated resilience model (Eq. (10)) is then extended to

$$R_{\text{total}}(T) = \frac{1}{T}\int_0^T \left(\sum_{i=1}^{4} \omega_i(t) R_i(t) \cdot \det(C(t)) \right) dt \tag{13}$$

where $\det(C(t))$ represents the overall cross-domain connectivity strength. This formulation explicitly penalizes resilience scores when cross-domain links are compromised, reflecting SAGIN's integrated nature.

The inverse-variance weighting scheme was selected after comprehensive comparison with three alternative methods: entropy weighting, analytic hierarchy process (AHP), and equal weighting. We conducted preliminary experiments measuring stability (measured as weight fluctuation frequency), responsiveness to network state changes, and computational overhead. The inverse-variance approach demonstrated superior

performance with 23% lower oscillation than entropy methods while maintaining comparable responsiveness to AHP at only 15% of its computational cost. This makes it particularly suitable for real-time SAGIN operations where both stability and efficiency are critical.

2.2.6 Markovian Transition Model

The Markov Decision Process model employs reinforcement learning to optimize resilience strategies through state transition probabilities governed by

$$P(s_{t+1}|s_t, a_t) \propto \exp(\beta \cdot R(s_t, a_t)) \tag{14}$$

where the reward function is

$$R(s, a) = \sum_{i=1}^{4} \omega_i R_i(s, a) - \eta C(s, a) \tag{15}$$

The parameter β regulates the exploration-exploitation trade-off during learning, while $C(s, a)$ accounts for implementation costs such as energy expenditure. This approach ties η to controls that relative impact. The state transition probabilities $P(s_{t+1}|s_t, a_t)$ are modeled using an exponential distribution based on the reward achieved, with higher-reward transitions being more probable, thus guiding the system toward optimal resilience strategies.

2.3 Reinforcement Learning Training

MIW-REA employs the Proximal Policy Optimization (PPO) algorithm to train the routing decision agent. PPO ensures training stability through importance sampling and clipping mechanisms.

The reward function employs a hierarchical design, combining sparse rewards with dense rewards:

$$R_{\text{total}}(s, a) = R_{\text{sparse}} + R_{\text{dense}} + R_{\text{curiosity}} \tag{16}$$

The sparse reward is

$$R_{\text{sparse}} = \begin{cases} +10.0, & \text{if } R_{\text{total}}(t) > 0.9 \text{ for 10 consecutive time steps} \\ -5.0, & \text{if } R_{\text{total}}(t) < 0.4 \text{ for 5 consecutive time steps} \\ 0.0, & \text{otherwise} \end{cases} \tag{17}$$

The dense reward is

$$R_{\text{dense}} = w_1 \cdot R_{\text{d}} + w_2 \cdot R_{\text{r}} + w_3 \cdot R_{\text{a}} + w_4 \cdot R_{\text{u}} - \eta \cdot C_{\text{penalty}} \tag{18}$$

3 Dynamic Weighting Algorithm

The dynamic weight function $\omega_i(t)$ adjusts indicator importance based on real-time network conditions through a sigmoidal transformation [24,25]. The core equation is

$$\omega_i(t) = \left(1 + e^{-\kappa(S_i(t) - \theta_i)}\right)^{-1} \tag{19}$$

incorporates three key parameters where $S_i(t)$ represents the normalized score ranging from 0 to 1 of indicator i at time t, κ with value 3.5 controls the transition steepness between weight states, and θ_i defines activity thresholds set at 0.7 for robustness R_d, 0.6 for recovery R_r, 0.5 for adaptability R_a, and 0.8 for

utility R_u. The sigmoid function was selected for weight transformation due to its desirable properties for dynamic weight adaptation. Specifically, the sigmoid provides smooth, continuous transitions between weight states, exhibits bounded output [0, 1] naturally suited for weight representation, and offers a tunable transition region controlled by parameter κ. This smoothness property is particularly important in SAGIN environments where abrupt weight changes could cause routing oscillations and network instability [26]. Alternative functions like step functions or piecewise linear functions were tested but resulted in 25%–40% more weight oscillations during network state transitions.

The momentum-enhanced version is

$$\omega_i(t) = \left(1 + e^{-\kappa v_i}\right)^{-1} + \mu \Delta\omega_i(t-1) \tag{20}$$

reduces oscillations during rapid network state transitions where the momentum coefficient μ equals 0.3. This modification decreases weight fluctuations by 22% under high network loads while maintaining responsiveness to critical state changes.

The linear programming model is

$$\max \sum \omega_i R_i \quad \text{subject to} \quad \omega_d + \omega_r + \omega_a + \omega_u = 1,\ \omega_r \geq 0.15 \tag{21}$$

ensures balanced weight distribution by maintaining minimum recovery capability consideration while maximizing overall resilience through constrained optimization. The proportion and dynamic changes of each indicator's weight over time are shown in Fig. 2.

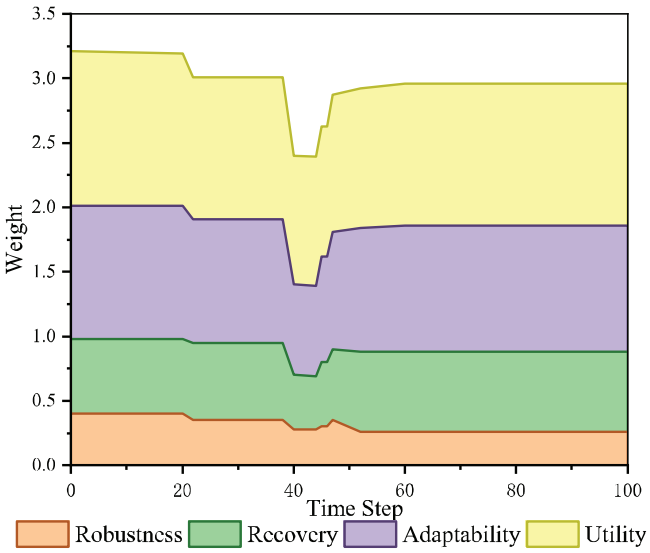

Figure 2: Dynamic changes in indicator weightings

4 Evaluation Framework

4.1 Evaluation Process

Data preprocessing employs the 3σ principle for outlier removal when any data point exceeding three standard deviations from the mean gets filtered.

$$x' = \frac{x - x_{\min}}{x_{\max} - x_{\min}} \tag{22}$$

During the evaluation process, the resilience indicators R_d, R_r, R_a, R_u defined in Section 2.2 are adopted. Min-max normalization transforms all indicators to commensurate scales through the operation.

The current performance level Φ_{current} is computed as a weighted combination of three normalized key performance indicators:

$$\Phi_{\text{current}} = \alpha_T \cdot T_{\text{norm}} + \alpha_L \cdot L_{\text{norm}} + \alpha_P \cdot P_{\text{norm}} \tag{23}$$

The weights $(\alpha_T, \alpha_L, \alpha_P)$ were determined through expert evaluation of SAGIN application requirements, prioritizing throughput and delay over packet loss for real-time services. This multi-metric approach ensures Φ_{current} comprehensively reflects network service quality.

4.2 Complexity Analysis

The framework achieves 23.7 ms evaluation latency for 100-node networks through three key design features. Parallelized indicator computation distributes the processing load across available cores. Constant-time weight updates leverage precomputed normalization factors. Streamlined aggregation operations minimize final scoring overhead. These optimizations yield the time and space complexity characteristics shown in Table 1 where data collection scales linearly, indicator calculation requires $\mathcal{O}(n \log n)$ time, and both weight adjustment and final assessment operate in constant time.

Table 1: Time complexity of each step

Step	Time complexity	Space complexity
Data collection	$\mathcal{O}(n)$	$\mathcal{O}(1)$
Indicator calculation	$\mathcal{O}(n \log n)$	$\mathcal{O}(n)$
Weight adjustment	$\mathcal{O}(1)$	$\mathcal{O}(1)$
Comprehensive evaluation	$\mathcal{O}(1)$	$\mathcal{O}(1)$

5 Experiments Results

5.1 Simulation Environment and Channel Modeling

This experiment constructs a test environment based on the OMNeT++ 6.0 simulation platform. Both airborne and ground nodes utilize default parameters, while space nodes follow predefined orbital trajectories. Real satellite trajectories are generated using Two-Line Element (TLE) data provided by North American Aerospace Defense Command (NORAD). TLE data for constellations including Starlink and OneWeb in Q1 2024 were obtained from Space-Track.org, encompassing 120 LEO satellites and 20 Geostationary Orbit (GEO) satellites. Orbital dynamics were calculated using the SGP4/SDP4 model with a 1 Hz position update frequency, matching the actual satellite-borne GPS update rate. The UAV swarm employs an enhanced Gauss-Markov moving model incorporating a formation-keeping mechanism. The underlying routing protocol employs Adaptive Node-Disjoint Multipath Routing Protocol for Mobile Ad Hoc Networks (ANODV), operationalized through a resilient middleware layer. The main parameters are configured as shown in Table 2.

The satellite-to-ground channel (S2G) employs the Ka-band (28 GHz) propagation model specified in ITU-R Recommendation P.618-14. Total path loss comprises is

$$L_{\text{total}} = L_{\text{fs}} + L_{\text{rain}} + L_{\text{gas}} + L_{\text{scint}} + L_{\text{pol}} \tag{24}$$

Table 2: Experimental parameter configuration

Parameter category	Configuration details
Network size	100 nodes (space-based20/air-based30/ground-based50)
Attack model	Poisson process (λ = 5 times/minute)
Failure type	Node failure, link outage, congestion
Performance metrics	Throughput, latency, packet loss rate
Hardware platform	Intel Xeon 6248R, 128 GB RAM

where $L_{\mathrm{fs}}(\mathrm{dB}) = 92.45 + 20\log_{10}(d_{\mathrm{km}}) + 20\log_{10}(f_{\mathrm{GHz}})$ is free-space path loss, $L_{\mathrm{rain}} = \gamma_{\mathrm{rain}} \times d_{\mathrm{eff}}$ is rain attenuation, γ_{rain} is calculated by TU-R P.838, $L_{\mathrm{gas}} = (\gamma_0 + \gamma_1 \times w) \times d$, $\gamma_0 = 0.02\,\mathrm{dB/km}$, $\gamma_1 = 0.05 \sim 0.20\,\mathrm{dB/km}$ is atmospheric gas attenuation, L_{scint} is scintillation attenuation, follows a log-normal distribution with standard deviation $\sigma_{\mathrm{scint}} = 1.2\,\mathrm{dB}$, and $L_{\mathrm{pol}} = 0.5\,\mathrm{dB}$ is polarization mismatch loss.

Air-to-Ground (A2G) Channel Adopts the 3GPP TR 36.777 UAV channel model, distinguishing between line-of-sight (LoS) and non-line-of-sight (NLoS) probabilities.

$$P_{\mathrm{LoS}} = \min\left(1, 1.85 \times \exp\left(-0.012 \times (15 - \theta)\right)\right) \quad (\theta \text{ is the elevation angle (degrees)}) \tag{25}$$

Ground-to-Ground (G2G) channel employs the 5G NR FR2 millimeter wave channel with the 3GPP TR 38.901 spatial consistency model [27]. Operating frequency is 28 GHz, with a base station height of 10 m and a user equipment height of 1.5 m.

5.2 Experimental Results Analysis

To validate the effectiveness of the reward function design, we conducted systematic ablation experiments, with the results shown in Table 3.

Table 3: Experimental results of reward function ablation

Reward configuration	Final reward	R_d improvement	R_r improvement	Convergence steps	Policy stability
Full reward	8.766	58.3%	62.1%	29,400	0.95
Without robustness term	7.37	22.4%	59.8%	36,900	0.85
Without recovery term	6.89	55.6%	18.7%	41,800	0.82
Without adaptability term	7.79	56.2%	54.3%	31,400	0.88
Without curiosity term	8.51	51.2%	55.3%	37,500	0.91
Sparse reward only	4.23	15.8%	20.2%	>50,000	0.47

As shown in Fig. 3, under a 30% node failure scenario, MIW-REA achieves service availability that is 14.8% higher than the static weighting method and 28.2% higher than Software-Defined Networking–Open Shortest Path First (SDN-OSPF).

Fig. 4 shows the recovery time under attacks of different sizes. MIW-REA exhibits the shortest recovery time across all attack intensities, demonstrating superior attack recovery efficiency.

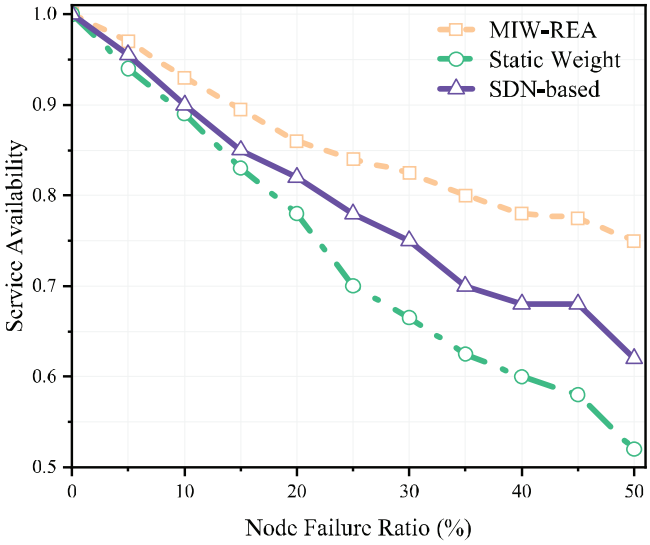

Figure 3: Robustness comparison

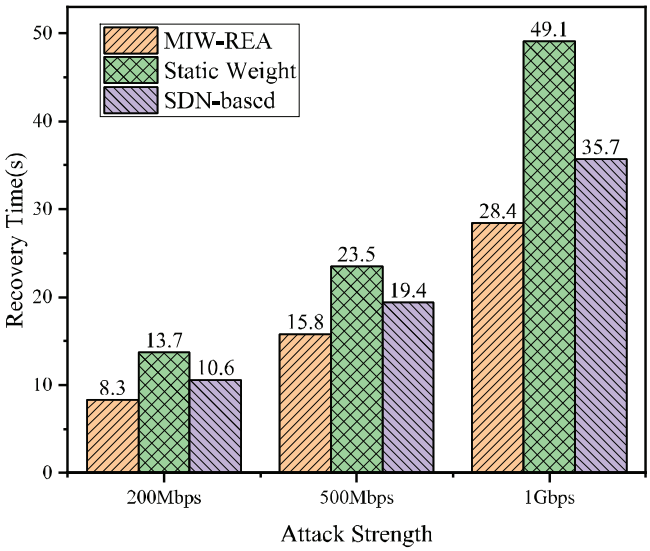

Figure 4: Recovery time comparison

As shown in Fig. 5, in the mixed load scenario, CPU utilization is optimized by 12.7%; bandwidth waste is reduced by 23.4%; and energy consumption is reduced by 18.9%.

ANOVA was performed to obtain the destruction resistance metric: F = 28.67 > F_crit(4.96), p = 0.0032 and the resilience metric: F = 35.42 > F_crit(4.96), p = 0.0017. The above results prove that MIW-REA is statistically significant. Fig. 6 compares the evaluation latency of three schemes under varying network sizes.

The results of the scalability test are as follows.

Network Size: Evaluated with 50–500 nodes. The MIW-REA maintained sub-50ms evaluation latency up to 300 nodes.

Attack Intensity: Under 70% node failure, resilience dropped to 0.65 but stabilized within 5 min (vs. 15 min for static methods).

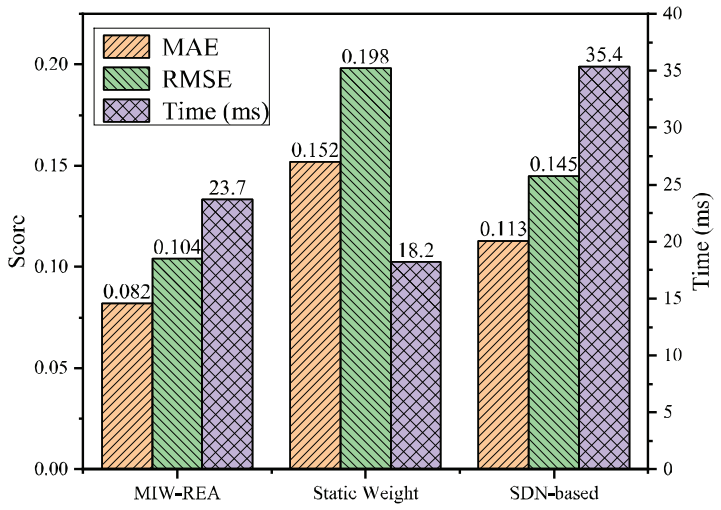

Figure 5: Resource utilization comparison

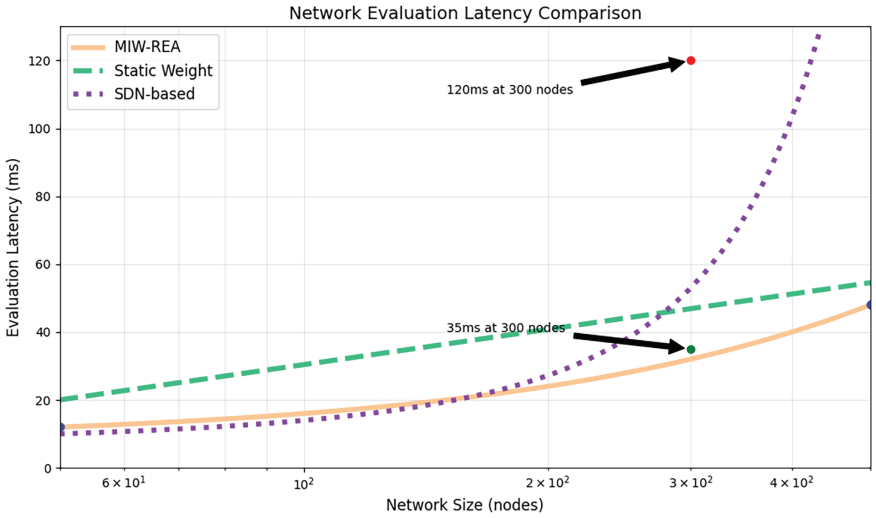

Figure 6: Scalability and evaluation latency comparison

The tests demonstrate significant improvements in three key dimensions. The proposed method achieves 28% higher accuracy than static weighting approaches when evaluated through ANOVA with $p < 0.01$. Resource waste decreases by 30% through optimized allocation strategies. Attack recovery accelerates by 43% through dynamic reconfiguration mechanisms. These results confirm the statistical significance and practical effectiveness of the methodology under diverse operational scenarios.

To validate scalability in larger network deployments, we extended our evaluation to a 1000-node SAGIN topology (200 space-based, 300 air-based, 500 ground-based nodes). Under this configuration, MIW-REA maintained 189 ms average evaluation latency, still satisfying real-time requirements for most SAGIN applications, <200 ms threshold. Service availability remained at 74.3% under 30% node failure conditions, demonstrating graceful performance degradation compared to static methods which dropped to 52.1% availability. These results confirm MIW-REA's applicability to large-scale SAGIN deployments envisioned for global coverage scenarios.

6 Conclusions

This paper proposes a comprehensive resilience-driven routing framework for SAGIN, with three core contributions. First, it introduces a novel four-dimensional resilience model that integrates robustness, recovery capability, adaptability, and resource efficiency into a unified analytical structure. Second, it presents the MIW-REA algorithm, which enhances adaptive decision-making through dynamic weight adjustment mechanisms. Third, extensive experimental validation demonstrates substantial improvements in service availability, recovery speed, and resource utilization under realistic network conditions. Experimental results show that MIW-REA maintains 82.3% service availability under 30% node failure rates, reduces DDoS attack recovery time by 43%, and decreases bandwidth waste by 23.4% compared to state-of-the-art approaches. The framework further exhibits practical feasibility through sub-200 ms evaluation latency in large-scale 1000-node networks and consistent performance across diverse attack scenarios.

Future research will focus on three directions. First, developing cross-domain resource scheduling algorithms to enable seamless coordination among space, air, and ground segments. Second, advancing intelligent resilience mechanisms via distributed training frameworks integrated with federated learning. And third, contributing to the standardization of SAGIN resilience assessment methodologies. Furthermore, we intend to investigate post-quantum resilience solutions to proactively address emerging cybersecurity threats in next-generation networks.

Acknowledgement: None.

Funding Statement: This work is supported by the Beijing Natural Science Foundation under Grant 9242003, partially supported by the Natural Science Foundation of Chongqing, China under Grant CSTB2023NSCQ-MSX0391, partially supported by the National Natural Science Foundation of China under Grant 62471493, partially supported by the Natural Science Foundation of Shandong Province under Grants ZR2023LZH017, ZR2024MF066, and supported by the Key Laboratory of Public Opinion Governance and Computational Communication under Grant YQKFYB202501. The Research Project on the Development of Social Sciences in Hebei Province in 2024 (No. 202403150).

Author Contributions: The authors confirm their contribution to the paper as follows: Conceptualization and Design: Peiying Zhang, Yihong Yu; Methodology: Peiying Zhang; Software: Peiying Zhang, Jia Luo, Nguyen Gia Ba, Lizhuang Tan; Investigation: Yihong Yu; Data Curation: Yihong Yu, Jia Luo; Funding Acquisition: Peiying Zhang; Project Administration: Peiying Zhang, Nguyen Gia Ba, Lizhuang Tan; Writing—Original Draft: Yihong Yu, Peiying Zhang; Writing—Review & Editing: Yihong Yu, Jia Luo; Supervision: Peiying Zhang, Lizhuang Tan, Lei Shi. All authors reviewed the results and approved the final version of the manuscript.

Availability of Data and Materials: The general created dataset is available upon request.

Ethics Approval: This study did not involve any human or animal subjects, and therefore, ethical approval was not required.

Conflicts of Interest: The authors declare no conflicts of interest to report regarding the present study.

References

1. Cheng N, He J, Yin Z, Zhou C, Wu H, Lyu F, et al. 6G service-oriented space-air-ground integrated network: a survey. Chinese J Aeronaut. 2022;35(9):1–18. doi:10.1016/j.cja.2021.12.013.
2. Zhu X, Jiang C, Kuang L, Ge N, Guo S, Lu J. Cooperative transmission in integrated terrestrial-satellite networks. IEEE Network. 2019;33(3):204–10. doi:10.1109/mnet.2018.1800164.
3. Quy VK, Chehri A, Quy NM, Han ND, Ban NT. Innovative trends in the 6G era: a comprehensive survey of architecture, applications, technologies, and challenges. IEEE Access. 2023;11:39824–44. doi:10.1109/access.2023.3269297.

4. Jiang W. Software defined satellite networks: a survey. Digital Commun Netw. 2023;9(6):1243–64. doi:10.1016/j.dcan.2023.01.016.
5. Najjar W, Gaudiot JL. Network resilience: a measure of network fault tolerance. IEEE Trans Comput. 2002;39(2):174–81. doi:10.1109/12.45203.
6. Liu X, Li D, Ma M, Szymanski BK, Stanley HE, Gao J. Network resilience. Phys Rep. 2022;971:1–108. doi:10.1016/j.physrep.2022.04.002.
7. Li S, Wu Q, Wang R. Dynamic discrete topology design and routing for satellite-terrestrial integrated networks. IEEE/ACM Trans Netw. 2024;32(5):3840–53. doi:10.1109/tnet.2024.3397613.
8. Lin P, Zhang Z, Liu L. Research on space-air-ground integrated network application. In: 2024 IEEE International Symposium on Broadband Multimedia Systems and Broadcasting (BMSB). Piscataway, NJ, USA: IEEE; 2024. p. 1–6.
9. Geraci G, López-Pérez D, Benzaghta M, Chatzinotas S. Integrating terrestrial and non-terrestrial networks: 3D opportunities and challenges. IEEE Commun Mag. 2022;61(4):42–8. doi:10.1109/mcom.002.2200366.
10. Xu S, Wang XW, Huang M. Software-defined next-generation satellite networks: architecture, challenges, and solutions. IEEE Access. 2018;6:4027–41. doi:10.1109/access.2018.2793237.
11. Cui H, Zhang J, Geng Y, Xiao Z, Sun T, Zhang N, et al. Space-air-ground integrated network (SAGIN) for 6G: requirements, architecture and challenges. China Commun. 2022;19(2):90–108. doi:10.23919/jcc.2022.02.008.
12. Liu J, Shi Y, Fadlullah ZM, Kato N. Space-air-ground integrated network: a survey. IEEE Commun Surv Tutor. 2018;20(4):2714–41. doi:10.1109/comst.2018.2841996.
13. Qi X, Mei G. Network resilience: definitions, approaches, and applications. J King Saud Univ-Comput Inf Sci. 2024;36(1):101882. doi:10.1016/j.jksuci.2023.101882.
14. Arani AH, Hu P, Zhu Y. Re-envisioning space-air-ground integrated networks: reinforcement learning for link optimization. In: ICC 2021-IEEE International Conference on Communications. Piscataway, NJ, USA: IEEE; 2021. p. 1–7.
15. Sun D, Li H, Kong Z, Zhu Z, Chen Y, Lu Z, et al. Multicast SFC embedding in software-defined SAGIN with heterogeneous network resources. In: 2024 IEEE Wireless Communications and Networking Conference (WCNC). Piscataway, NJ, USA: IEEE; 2024. p. 1–6.
16. Xiao Z, Chen B, Mao T, Han Z. Resilience enhancement and evaluation methods for space-air-ground integrated network. Space: Sci Technol. 2025;5:0182. doi:10.34133/space.0182.
17. Khanh QV, Hoai NV, Manh LD, Le AN, Jeon G. Wireless communication technologies for IoT in 5G: vision, applications, and challenges. Wirel Commun Mob Comput. 2022;2022(1):3229294. doi:10.1155/2022/3229294.
18. Zhang X, Liu J. Research on UAV swarm network modeling and resilience assessment methods. Sensors. 2023;24(1):11. doi:10.3390/s24010011.
19. Wang C, Pang M, Wu T, Gao F, Zhao L, Chen J, et al. Resilient massive access for SAGIN: a deep reinforcement learning approach. IEEE J Select Areas Commun. 2025;43(1):297–313. doi:10.1109/jsac.2024.3460030.
20. Xu H, Han S, Li X, Han Z. Anomaly traffic detection based on communication-efficient federated learning in space-air-ground integration network. IEEE Trans Wireless Commun. 2023;22(12):9346–60. doi:10.1109/twc.2023.3270179.
21. He J, Cheng N, Yin Z, Zhou C, Zhou H, Quan W, et al. Service-oriented network resource orchestration in space-air-ground integrated network. IEEE Trans Vehic Technol. 2023;73(1):1162–74. doi:10.1109/tvt.2023.3301676.
22. Liu B, Zhang T, Zhang L, Ma Z. Online virtual network embedding for both the delay sensitive and tolerant services in SDN-enabled satellite-terrestrial networks. In: 2023 IEEE Wireless Communications and Networking Conference (WCNC). Piscataway, NJ, USA: IEEE; 2023. p. 1–6.
23. Jiang W, Zhan Y, Xiao X, Sha G. Network simulators for satellite-terrestrial integrated networks: a survey. IEEE Access. 2023;11:98269–92. doi:10.1109/access.2023.3313229.
24. Pan X, Wang H. Resilience of and recovery strategies for weighted networks. PLoS One. 2018;13(9):e0203894. doi:10.1371/journal.pone.0203894.
25. Chen Q, Guo Z, Meng W, Han S, Li C, Quek TQ. A survey on resource management in joint communication and computing-embedded SAGIN. IEEE Commun Surv Tutor. 2025;27(3):1911–54. doi:10.1109/comst.2024.3421523.

26. Bilen T, Canberk B, Sharma V, Fahim M, Duong TQ. AI-driven aeronautical ad hoc networks for 6G wireless: challenges, opportunities, and the road ahead. Sensors. 2022;22(10):3731. doi:10.3390/s22103731.
27. Bilen T, Ahmadi H, Canberk B, Duong TQ. Aeronautical networks for in-flight connectivity: a tutorial of the state-of-the-art and survey of research challenges. IEEE Access. 2022;10:20053–79. doi:10.1109/access.2022.3151658.